Effects of Internal Hydrogen on Fatigue Strength of Commercially Pure Titanium

Hideaki Nishikawa [1, a], Yasuji Oda [2,b] and Hiroshi Noguchi[2,c]

[1] Graduate School of Kyushu University, 744 Moto-oka, Nishi-ku, Fukuoka 819-0395, Japan

[2] Faculty of Engineering, Kyushu University, 744 Moto-oka, Nishi-ku, Fukuoka 819-0395, Japan

[a]nishikawa@mech.kyushu-u.ac.jp, [b]oda@mech.kyushu-u.ac.jp, [c]nogu@mech.kyushu-u.ac.jp.

Keywords: Commercially pure titanium, Fatigue, Hydrogen, Hydride.

Abstract. Commercially Pure Titanium (CP-Ti) usually contains a few tens of ppm hydrogen. In order to investigate the effect of such internal hydrogen on the fatigue characteristics, rotating bending fatigue tests were carried out on two kinds of specimen with different hydrogen contents: one contains 34 ppm but the other 3 ppm. The amount of internal hydrogen was controlled by changing the annealing conditions. The fatigue process was successively observed by a replication technique. The higher hydrogen content specimen showed a longer fatigue life, longer crack initiation life and higher fatigue limit than those of the lower hydrogen specimen. No specimen showed any particular fatigue crack growth behavior related to hydrogen content, whereas the crack initiation behavior differed somewhat. The fatigue-crack initiation site of the higher hydrogen content specimen with a longer fatigue life preferred the interior of a grain. On the other hand, that of the lower hydrogen specimen preferred the neighborhood of a grain boundary.

Introduction

Titanium and its alloys have been widely used for structural components because of their superior specific strength and environmental resistance compared with other metallic materials. However, titanium is a very active metal, therefore, not only oxygen and nitrogen but also hydrogen could be readily introduced into the material during manufacturing; these components affect the strength of titanium and its alloys. The effects of these components on the mechanical properties of commercially pure titanium have been long investigated. On the basis of the results, the hydrogen content in CP-Ti is controlled so as not to exceed 150 ppm[1]. However, this value seems to be selected mainly on the basis of the tensile and impact properties[2], which are governed predominantly by the hydride formed when the content of internal hydrogen exceeds its solution limit. Hydrogen is known to have detrimental effects on the strength of many metallic materials not forming any hydride. CP-Ti usually contains a few tens of ppm hydrogen. In the case of fatigue, such a small amount of hydrogen may exert the complex effects on the fatigue behavior of CP-Ti through the presence of hydride and solution-state hydrogen. Until now, there have been few reports concerning the effects of such a small amount of internal hydrogen on the fatigue behavior of CP-Ti[3,4].

In this study, two kinds of specimen with different hydrogen contents were prepared, and the effects of internal hydrogen usually contained in CP-Ti on the fatigue strength of this material are discussed on the basis of the results of rotating bending fatigue tests, successive observations of crack initiation and propagation behavior by a replication technique, and observation of fracture surfaces.

The material, specimen and the testing method

Material and specimen. The material used in this study was a CP-Ti rod (JIS H 4650 class 2) with a diameter of 14 mm. Table 1 lists the chemical composition of the material as-received. It contains 20 ppm hydrogen. Two kinds of specimen with different hydrogen contents were prepared. The amount of internal hydrogen was controlled by changing the annealing conditions: in air or in a vacuum. Figure 1 shows the procedure for preparing specimens. The required properties for a couple of specimens are as follows.

1) Reduce the hydrogen content close to 0 ppm (Low hydrogen specimen).
2) Preserve the hydrogen content as-received (High hydrogen specimen).
3) Minimize the differences in any other characteristics between 1) and 2) except hydrogen content.

Conceivable difficulties to achieve these objectives are the adsorption of oxygen and hydrogen when annealing in the furnace. To avoid these difficulties, following characteristics of the entry and diffusion of oxygen and hydrogen were considered.

i) Diffusion coefficient of oxygen in CP-Ti is relatively small at elevated temperature[5].
ii) Oxide film at the surface of CP-Ti acts as a barrier against oxygen and hydrogen[6].
iii) Diffusion coefficient of hydrogen in CP-Ti is very large at elevated temperature.

When preparing a low hydrogen specimen, internal hydrogen desorbed from the cleaned surface of CP-Ti by annealing at 830 °C for 24 hours in a vacuum. When preparing high hydrogen specimen, annealing at 830 °C for 24 hours in air thicken the oxide film and the diffusion layer of oxygen. However, a specimen having the same oxygen content as-received material can be made by removing the oxide film and the diffusion layer.

Table1 Chemical composition (mass%)

C	Si	Cr	Fe	Ni	N	O	H	Ti
0.008	0.007	0.008	0.058	0.009	0.005	0.116	0.002	bal.

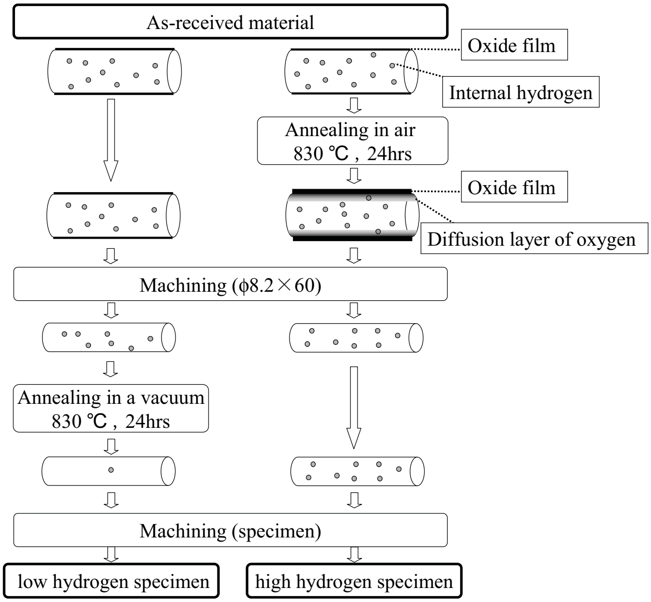

Fig. 1 Procedure for preparing specimens

In order to make sure whether the specimens achieve the objectives or not, the amount of contents of hydrogen and oxygen were investigated.

Figure 2 shows Thermal Desorption Spectrometer (TDS) profiles of hydrogen for two kinds of specimen. A high hydrogen specimen annealed in air contains 34ppm but a low hydrogen specimen annealed in a vacuum contains 3ppm.

Internal oxygen content was also measured with Non Dispersive Infrared Red Analyzer (NDIR), whether oxygen inside the specimen increases when annealing in air. Results of both kinds of specimen showed the same value each other; 0.13 mass%, which is also the same as-received material.

Figure3 shows the photographs of microstructure of each specimen. Average grain size of a high hydrogen specimen is about 316μm and a low hydrogen specimen also 322μm. Grain size became lager during annealing (Average grain size of as-received material is about 50 μm). There are a few reports that the effect of grain size on the qualitative behavior of the fatigue crack initiation does not appear[7,8]. In addition, acicular hydrides are seen in the interior of a grain of a high hydrogen specimen.

Small gaps between these results and required properties exist, however a couple of specimens are suitable for the comparison of tests on the different hydrogen specimens.

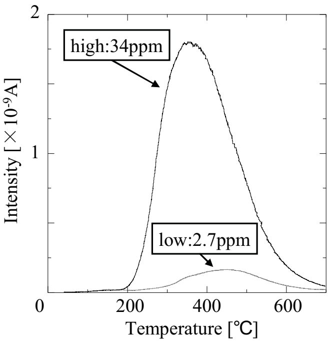

Fig. 2 TDS profiles for both specimens;
high: high hydrogen specimen,
low: low hydrogen specimen.

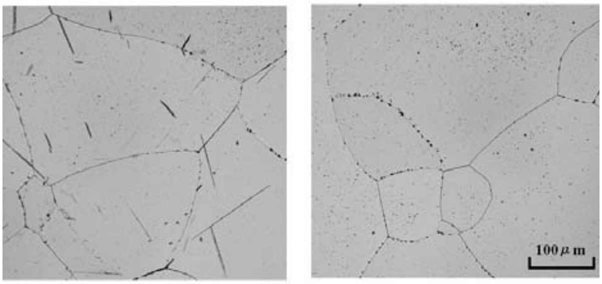

(a) High hydrogen specimen (b) Low hydrogen specimen

Fig. 3 Microstructures for both specimens.

Testing method. The testing machine is Ono-type rotating bending fatigue machine with a capacity of 15 N･m and a testing rate of 3000 rpm. The shape and dimensions of a specimen are shown in Figure 4. A shallow circular notch with a radius of 20 mm is introduced at the center to limit the area under observation of fatigue behavior. The stress concentration factor of the notch is approximately 1.03, therefore it can be considered that the specimen behaves as a plain specimen. The specimen surface was finally buff-polished to make it easy to observe the changes in the surface state. The fatigue process was successively observed using a replication technique. After fatigue tests, fracture surfaces were observed with a Scanning Electron Microscope (SEM).

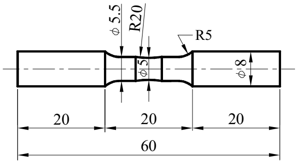

Fig. 4 Shape and dimensions of specimen (in mm).

Result

Fatigue test. Figure 5 shows the *S-N* diagram. The symbol ▲ represents the fatigue life of a high hydrogen specimen with 34 ppm hydrogen content, the symbol ■ of a low hydrogen specimen with 3 ppm. A high hydrogen specimen shows a longer fatigue life and a higher fatigue limit than the low hydrogen specimen. N_i represents the number of cycles to crack initiation conveniently defined as formation of a micro-crack with a length of a few micron meter. The symbol △ represents the initiation life of a high hydrogen specimen, the symbol □ of a low hydrogen specimen. It seems that a high hydrogen specimen show a longer crack initiation life than a low hydrogen specimen. When the applied stress amplitude is equal to the fatigue limit, no microcracks are observed on the specimen after 10^7 cycling of stress under an optical microscope. Therefore, the fatigue limit is determined by the limit of a microcrack initiation.

Figure 6 shows the crack growth plots. Figure 6 (a) shows those of all specimens. The fatigue crack growth life does not show the obvious difference related to hydrogen content. Figure 6 (b) shows the crack growth plots at relatively higher stress amplitude 230 MPa. The difference of fatigue life between both specimens is not due to the difference of crack growth life but due to the difference of crack initiation life. At lower stress amplitude, the number of cycles to crack initiation and growth to a micro-crack scattered. Therefore, it seemed that the fatigue lives have not clear relative tendencies between both kinds of specimens at lower stress.

The results described above suggest that the difference in the fatigue strength between two kinds of specimen is caused by the differences in the crack initiation behavior. Therefore, the crack initiation behavior was observed in each specimen.

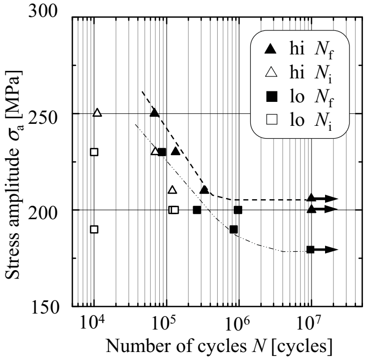

Fig. 5 *S-N* diagram. hi: high hydrogen specimen. lo: low hydrogen specimen.
N_i: Number of cycles to micro-crack initiation. N_f: Number of cycles to failure.

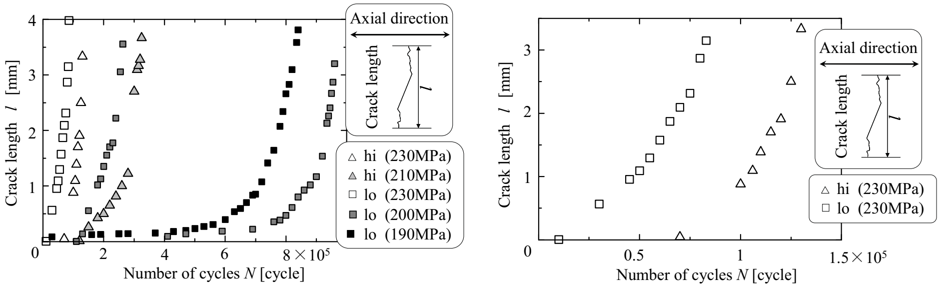

(a) All specimens (b) At σ_a=230MPa

Fig. 6 Crack growth plots. hi: high hydrogen specimen. lo: low hydrogen specimen.

Figure 7 shows the surfaces of both kind of specimen fatigued up to $N \simeq N_f$ at σ_a=230 MPa. In the high hydrogen specimen, there were 4 fatigue cracks in total, but in the low hydrogen specimen, there were 20 ~ 30 fatigue cracks. The resistance to crack initiation differs depending on hydrogen content.

Figure 8 shows the crack initiation process of both specimens at 230 MPa, and Figure 9 shows those slightly above the fatigue limits. At σ_a=230 MPa, cracks in the low hydrogen specimen initiate along slip bands near a grain boundary. On the other hands, in the high hydrogen specimen, cracks initiate inside grains. At the stress amplitude near the fatigue limit, cracks in both specimens initiate inside the grains.

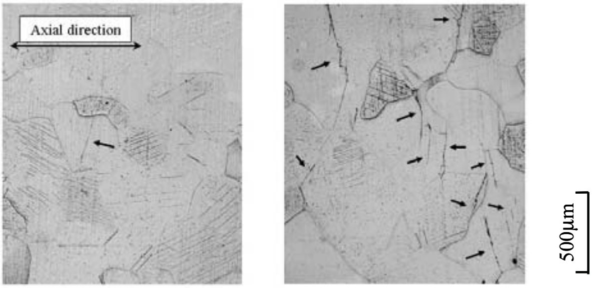

(a) (b)

Fig. 7 Surfaces of specimens at $N \simeq N_f$, σ_a=230 MPa: (a) high hydrogen specimen; $N_f=13\times10^4$, (b) low hydrogen specimen; $N_f=8.6\times10^4$. Arrows indicate microcracks.

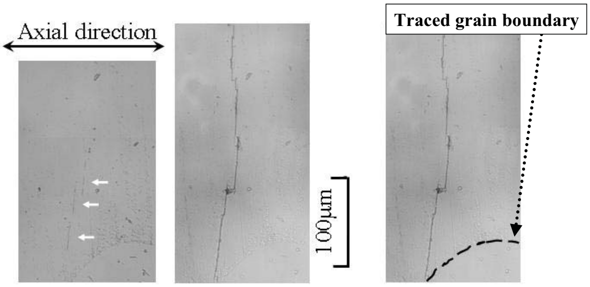

(a-1) $N=7\times10^4$ (a-2) $N=1\times10^5$ (a-3) Grain boundary traced in (a-2)

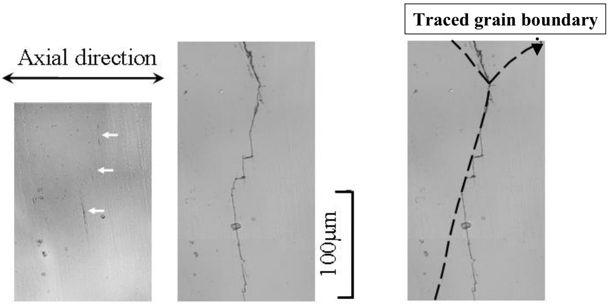

(b-1) $N=1\times10^4$ (b-2) $N=3\times10^4$ (b-3) Grain boundary traced in (b-2)

Fig. 8 Fatigue crack initiation process at σ_a =230 MPa: (a) high hydrogen specimen; $N_f=13\times10^4$, (b) low hydrogen specimen; $N_f=8.6\times10^4$. Arrows indicate microcracks.

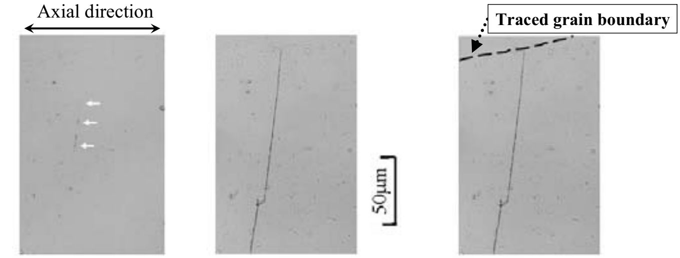

(a-1) N=1.2×10^5 (a-2) N=1.5×10^5 (a-3) Grain boundary traced in (a-2)

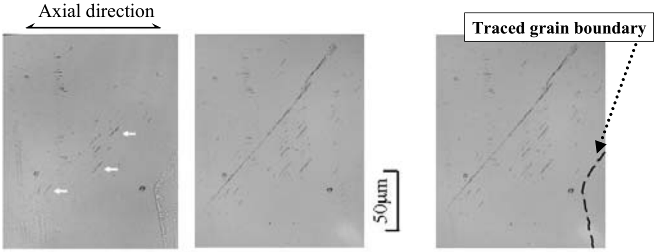

(b-1) N=2×10^5 (b-2) N=5×10^5 (b-3) Grain boundary traced in (b-2)

Fig. 9 Fatigue crack initiation process near the fatigue limit: (a) high hydrogen specimen; N_f=3.3×10^5, σ_a=210 MPa, (b) low hydrogen specimen; N_f=9.6×10^5, σ_a=200 MPa. Arrows indicate microcracks.

Fracture surface. In order to investigate the characteristics of crack initiation and early stage crack growth, the fracture surfaces of the specimens (a) and (b) shown in Figure 9 were observed.

Figure 10 shows low magnification views of the fracture surfaces corresponding to Figures 9 (a) and (b). Figure 11 (a-1) and (b-1) are the magnified views of crack initiation sites (A) shown in Figure (10). Between arrows correspond to the same region shown in the photographs (a-2) and (b-2) of the specimen surfaces. However, the fracture surface (b) shows only a part of the crack shown in Figure 10 (b) because of branching of the crack after (b-3) at the right arrow. Figure 12 shows the magnified views of early stage of crack growth corresponding to (B) s in Figure 10 (a) and (b).

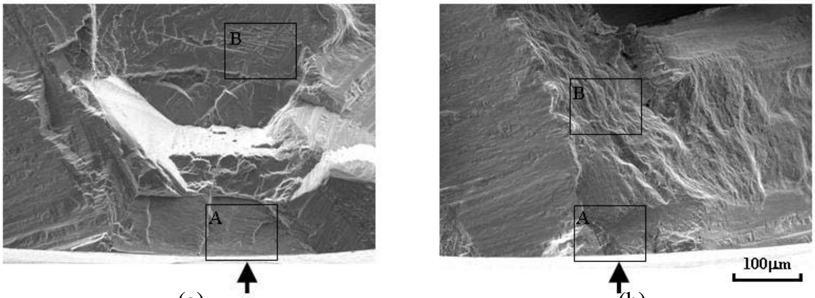

(a) (b)

Fig. 10 SEM images of fracture surfaces corresponding to Figure 9: (a) high hydrogen specimen; (b) low hydrogen specimen. Arrows on the specimen surfaces show crack initiation sites. Magnified views of (A) and (B) are shown in Figures 11 and 12.

General fracture surface morphology of both specimens appears crystallographic feature as shown in Figure 10. Fracture surfaces at the vicinity of crack initiation site of both specimens do not show significantly difference in morphology. However, the fracture surfaces of early stage of crack growth are rather different; that of the low hydrogen specimen revealed more ductile morphology shown in Figure 12 (b) than the other. Difference in the internal hydrogen content of both specimens is conceivable possibility of the difference in the morphologies, however apparent evidence related to hydrogen content was not observed.

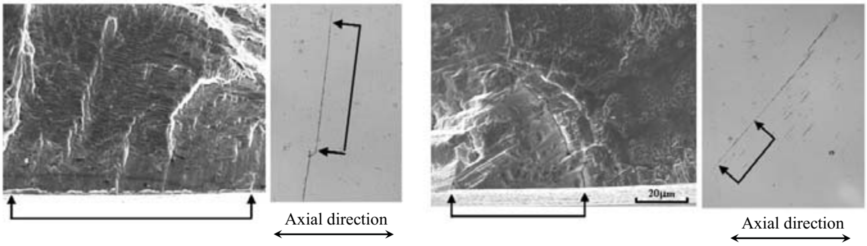

(a-1) (a-2) (b-1) (b-2)

Fig. 11 Enlargement of area A of Fig. 10: (a) high hydrogen specimen; (b) low hydrogen specimen.

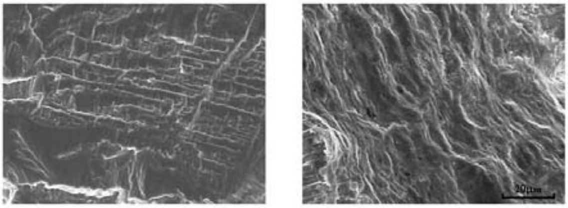

(a) (b)

Fig. 12 Enlargement of area B of Fig. 10: (a) high hydrogen specimen; (b) low hydrogen specimen.

Discussion

The results described above are summarized as follows.

1) Fatigue strength of a high hydrogen specimen is higher than that of a low hydrogen specimen.
2) The resistance to the initiation of a crack of a high hydrogen specimen is higher than that of a low hydrogen specimen. The crack growth behavior of two kinds of specimen did not show apparent difference related to hydrogen content. However, the fracture surfaces at the early stage of crack growth were rather different between two kinds of specimens.
3) The fatigue-crack initiation site differed depending on hydrogen content; inside a grain in a high hydrogen content specimen, at the neighborhood of a boundary in a low hydrogen content specimen.

It is considered that the hydrogen in CP-Ti exists partially in the solution state but mostly as hydrides. There is the possibility that both states of hydrogen affect the fatigue strength. In this study, the effects of the two states of hydrogen could not be distinguished. However, hydride is reported to be brittle, and harder than the base material [10]. In addition, expansion during hydride formation[11] causes the stress and deformation in base material [12]. Thus hydride or base material near a hydride is considered to exhibit some resistance to slip deformation of the base material. In addition, it is considered that the hydride segregate near the grain boundary. It seems that the effect of hydrides is predominant in this study.

Conceivable possibilities of the effect of hydride on slip behavior related to crack initiation are as follows.

- Hydride at the grain boundary restrains slip deformation near the grain boundary.
- Hydride interior the grain restrains slip deformation.

However, the phenomenon that hydride suppresses slip behavior has not been directly observed. It will be the subject of future studies.

In addition, hydrogen in the hydride cannot diffuse in the material; that is, hydride is not a factor of crack growth acceleration. Thus, the hydrogen usually contained in CP-Ti is advantageous for enhancing fatigue strength, within the limits of this study. However, the situation is different with higher mean stress, impact load or rather higher temperature, which cause cracking hydride or melting of the hydride respectively.

Summary

In order to investigate the effect of the internal hydrogen usually contained in CP-Ti on the fatigue characteristics, rotating bending fatigue tests were carried out on two kinds of specimens with different hydrogen contents: one contains 37 ppm hydrogen, the other 3 ppm hydrogen. The main results are as follows.

(1) The higher hydrogen content specimen showed a longer fatigue life, longer crack initiation life and higher fatigue limit than those of the lower hydrogen specimen. These phenomena are due to the difference in crack initiation.
(2) It is considered that the cause of the above-described result is the ability of hydride to inhibit slip.
(3) The small amount of internal hydrogen usually contained in CP-Ti behaves rather advantageous to the fatigue strength within the limits of this study.

References

[1] M.J. Donachie, jr. TITANIUM : A Technical Guide, ASM International, (1988), pp.8-9, 27-28, 209-218.

[2] C.J.Beevers., M.R.Warren.,and D.V.Edmond., Journal of the Less-Common Metals, Vol. 14(1968), pp.387-396.

[3] C.Q.Chen., and S.X.Li., Materials Science and Engineering A, Vol.387-389(2004), pp.470-475.

[4] C.Q.Chen., S.X.Li., and K.Lu., Acta Materialia, Vol. 51(2003), pp.931-942.

[5] K.Asaoka., and K.Maejima., Dental Materials journal, Vol. 24, No6(2005), pp.439-445.

[6] F.Watari., and F.Nishimura., Dental Materials journal, Vol. 10, No2(1991), pp.266-274.

[7] K.Takao., M.Sogho., and K.Matsumoto., Transactions of JSME, Series A, Vol. 52, No.484(1986), pp.2574-2778.

[8] K.Tokaji., T.Ogawa., and K.Ohya., Transactions of JSME, Series A, Vol. 58, No.546(1992), pp.178-185.

[9] H.Numakura and M.Koiwa., Acta metal. Vol. 32, No.10, (1984), pp.1799-1807.

[10] J.J.Xu, H.Y.Cheung., and S.Q.Shi., Journal of Alloys and Compounds, Vol. 436(2007), 82-85.

[11] M.I.Luppo, A. Politi, and G. Vigna., Hydrides in a-Ti: Charactarization and effect of applied external stress, Acta metal. Vol. 53, (2005), pp.4987-4996.

[12] N. E. Paton, and J. C. Williams, Hydrogen in Metals, edited by M. Bernstein and A. Thompson, ASM, (1974), p. 409.